Gd@C82: Origin of the Antiferromagnetic Coupling between Endohedral Gd and the Free Spin on the Carbon Cage†

ARTICLE *in* THE JOURNAL OF PHYSICAL CHEMISTRY C · DECEMBER 2009

Impact Factor: 4.77 · DOI: 10.1021/jp906243v

2 AUTHORS, INCLUDING:

Ali Sebetci
Mevlana University
24 PUBLICATIONS **259** CITATIONS

SEE PROFILE

$Gd@C_{82}$: Origin of the Antiferromagnetic Coupling between Endohedral Gd and the Free Spin on the Carbon Cage†

Ali Sebetci*,‡ and Manuel Richter*

IFW Dresden, P.O. Box 270116, D-01171 Dresden, Germany

Received: July 2, 2009; Revised Manuscript Received: November 21, 2009

The structure and magnetic ground state of the endohedral metallofullerene $Gd@C_{82}$ is confirmed by relativistic density functional calculations. The experimentally observed reduction of the magnetic moment of $Gd@C_{82}$ with respect to that of a free Gd^{3+} ion is explained by a small hybridization between unoccupied Gd-4f states and carbon-π states, resulting in a presumably generic antiferromagnetic coupling of the Gd-4f spin with the remaining unpaired spin in the hybridized molecular orbital.

I. Introduction

Rare-earth (RE) based metallofullerenes like $RE@C_{60}$,[1] $RE@C_{82}$,[2] and $RE_3N@C_{80}$[3] have recently attracted a wide interest in chemistry, physics, and biology. Metallofullerenes are promising, for example, for photoelectrochemical cell[4] and for molecular memory[5,6] applications as well as for the use in spintronics devices.[7] Another important field of application might emerge in the use of magnetic, in particular Gd-containing, metallofullerenes as contrast agents in magnetic resonance imaging.[1−3,8] Therefore, endohedral monometallofullerenes of type $RE@C_{82}$, beside others, have been intensively studied during the past decade.[9−17] Despite the considerable number of investigations published, the interaction between the metal atom and the carbon cage deserves further clarification. In particular, the electronic origin of the observed magnetic ground state of $Gd@C_{82}$ is not understood so far.

Let us first summarize the status of structural investigations of $RE@C_{82}$. The cage structures of $Sc@C_{82}$[18] and $La@C_{82}$[19] have been determined by synchrotron radiation powder diffraction combined with data analysis using the maximum entropy method (MEM). Both molecules have C_{2v} symmetry with RE atoms located at an off-center position adjacent to a carbon six-membered ring.[18,19] This structure has been confirmed by ^{13}C NMR spectroscopy.[20] The similarity in UV/vis/NIR spectra of 10 kinds of $RE@C_{82}$ (RE = La, Ce, Pr, Nd, Gd, Tb, Dy, Ho, Er, and Lu)[21] dissolved in toluene suggests that $Gd@C_{82}$ possesses C_{2v} symmetry as well. In addition, an extended X-ray absorption fine structure (EXAFS) study indicated a position of the Gd ion in the C_{82} cage above a carbon hexagon[22] like the Sc and La cases. However, in a later experimental study, Nishibori et al.[23] suggested, on the basis of synchrotron radiation powder structure MEM analysis, that the Gd atom would be located in the vicinity of the C−C double bond on the same C_2 molecular axis of the C_{82} cage but opposite to the six-membered ring where Sc and La atoms in $Sc@C_{82}$ and $La@C_{82}$ are known to be placed.

On the theoretical side, it is reported in an earlier density functional theory (DFT) study[11] that the most stable structure of $La@C_{82}$ has C_{2v} symmetry with La strongly bonded to a hexagonal ring. In this study, structural relaxation of $Gd@C_{82}$ with different initial positions of the Gd atom in the cage was not considered. Later, Senapati et al.[24−26] reported scalar relativistic DFT calculations with effective core potentials (ECP) that did not agree with the MEM/Rietveld-based X-ray synchrotron powder diffraction structure of Nishibori et al.[23] They found the most stable position of the Gd atom adjacent to the C−C double bond but not on the C_2 molecular axis of the C_{82} cage.[26] Finally, the disagreement on the position of the Gd ion in the cage has been solved both theoretically and experimentally: Mizorogi and Nagase[27] performed further DFT calculations and revealed that the so-called anomalous structures with Gd close to the double bond are unstable and do not correspond to energy minima. Also, Liu et al.[28] showed by an X-ray absorption near-edge structure (XANES) study that Gd indeed is situated above the hexagon on the C_2 axis, like La and Sc in the respective cases.

Effective magnetic moments μ_{eff} of $RE@C_{82}$ metallofullerenes have been measured by employing superconducting quantum interference device (SQUID) magnetometry for RE = La, Gd[9] and RE = Gd, Tb, Dy, Ho, Er,[12] by soft X-ray magnetic circular dichroism (XMCD) spectroscopy for RE = Gd, Dy,[17] and by XMCD combined with X-ray absorption spectroscopy for RE = Gd, Dy, Ho.[15] It was found that the effective moments are significantly smaller than those of the corresponding free RE^{3+} ions. The amount of the observed reduction is different for each metallofullerene with a general trend that the higher the orbital momentum, the larger the magnitude of the reduction.[12] In particular, the measured values of 6.91 μ_B[12] and 6.8 ± 0.5 μ_B[17] for $Gd@C_{82}$, which were obtained by fitting the experimental data to a Curie−Weiss law, correspond to about 13% reduction compared to the theoretical effective moment of 7.94 μ_B of the free trivalent Gd ion. The case of Gd is simpler than that of other RE, since the Gd magnetic moment is almost completely spin-dominated. Thus, the effective moment can be related to the allowed spin multiplicities, $M = 2S + 1$, being even for Gd^{3+} and odd for free $Gd@C_{82}$. Indeed, $\mu_{eff} = 7.94\ \mu_B$ corresponds to $M = 8$ (Gd^{3+}) while $\mu_{eff} = 6.93\ \mu_B$ would correspond to $M = 7$ if a vanishing orbital contribution is presumed.

Senapati et al.[24] calculated the total DFT energies of $Gd@C_{82}$ for different spin multiplicities. They concluded that $M = 7$, an antiferromagnetic arrangement of the Gd 4f-electrons and the remaining unpaired electron, is the lowest magnetic state,

† PACS numbers: 71.20.Tx, 73.22.-f, 75.75.+a.

* To whom correspondence should be addressed. E-mail: m.richter@ifw-dresden.de.

‡ Current affiliation: Department of Computer Engineering, Zirve University, Gaziantep 27260, Turkey. E-mail: alisebetci@zirve.edu.tr.

10.1021/jp906243v
Published on Web 12/11/2009

followed by $M = 9$, a related ferromagnetic arrangement. This is in agreement with the experimental result by Furukawa et al.[14] The latter authors estimated the energy difference between the two states to be about 2 meV[14] by comparing high-field/high-frequency ESR data with model Hamiltonian simulations. One should note, however, that this estimate is in contrast to the SQUID susceptibility data of Huang et al., who find Curie−Weiss behavior with an effective moment of 6.91 μ_B up to a temperature of 250 K.[12] Such a temperature-independent effective moment points to a gap between the $M = 7$ ground state and a state with larger M of more than 25 meV.

Later, using the GAUSSIAN 03 code and a hybrid exchange correlation functional (B3LYP), Mizorogi and Nagase[27] found in contradiction with experiment, that the $M = 9$ state would be 0.4 meV more stable than the $M = 7$ state. This result also contradicts the previous calculation by Senapati et al.,[24] who, however, obtained their conclusion only for one of the anomalous positions.[25,26] In addition, we note that in all previous calculations on Gd@C_{82} the Gd-4f electrons were treated without any on-side correlation correction. Such corrections are obligatory for a decent DFT description of 4f states in most rare-earth elements[29] and have been applied, for example, to the Gd-4f states of Gd@C_{60}[30] recently.

The aim of this work is to investigate the origin of the observed $M = 7$ ground state of Gd@C_{82} theoretically. Starting from local spin density (LSDA) and generalized gradient approximations (GGA), we include a so-called on-site correlation correction, spin−orbit coupling, and noncollinearity effects in the DFT calculations. These effects were not considered in any of the above-mentioned previous DFT approaches to Gd@C_{82}.

In a recent quantum chemical model approach, Mirone[31] investigated the combined effect of spin−orbit interaction and anisotropic hybridization on the low-temperature field dependence of magnetization of Gd@C_{82}. With an appropriate choice of the model parameters, the measured low-temperature deviation of the isothermal magnetization from a Brillouin function,[12,15] which is usually explained by antiferromagnetic intermolecular interaction and manifests itself in a nonzero Weiss temperature, could be explained by magnetocrystalline anisotropy (on the order of 1 meV) in the disordered powder sample.[31] Here, we will not consider magnetic anisotropy but rather focus on the spin magnetic ground state of the free molecule.

II. Computational Details

Three DFT codes have been used in our investigation: NWChem,[32] FPLO-7.28,[33] and OpenMX.[34,35] This was necessary as none of the codes includes all the technical prerequisites needed.

Geometry optimization has been performed with the program package NWChem in scalar-relativistic mode without using any on-site correlation correction. The effect of on-site correlation corrections on the geometry has been studied by OpenMX. It turns out that both methods give very similar results, but the OpenMX geometry data slightly deviate from the experimentally observed C_{2v} symmetry. Thus, we used the NWChem geometry data in the further calculations despite the fact that they were obtained by calculations without on-site correlation corrections. The magnetic ground state has been investigated using on-site correlation corrected calculations with the FPLO code in scalar-relativistic mode. We also carried out the final analysis of the electronic structure with this code in order to clarify the origin of the observed antiferromagnetic coupling. In addition, the effect of spin−orbit coupling and noncollinear magnetic moments has been checked with the OpenMX code.

In the calculations with NWChem, the hybrid functional B3LYP[36] has been chosen as the exchange-correlation functional, since this functional is known to provide geometries close to experiment in carbon systems. The scalar-relativistic ECP and basis set developed by Cundari and Stevens[37] were used for Gd, where the 46 inner electrons are replaced by the ECP and the outer 4f5s5p5d6s electrons are treated in the valence region. The split-valence 3-21G* and 6-31G* basis sets were used for C.

The program package OpenMX[34,35] is based on norm-conserving pseudopotentials[38] and pseudoatomic localized basis functions. In the calculations with OpenMX, the same outer electrons of the Gd atom as in the NWChem calculations were treated as valence electrons. The pseudoatomic orbitals were constructed by minimum basis sets (two s, one p, one d, and one f for Gd, and one s and one p for C) within 8.0 Bohr radii cutoff radius of the confinement potential for Gd and 5.0 Bohr radii for C. The GGA+U approach in the OpenMX-implementation[39] was applied in the atomic limit version in order to describe the correlated behavior of the Gd-4f shell. A value of $U - J = 7.2$ eV was used and the GGA functional was parametrized according to PBE.[40] A value of $U = 7.6$ eV was recently used in a similar calculation for Gd@C_{60}.[30] The cutoff energy for the real-space grid integration in the construction of the density matrix elements[35] has been chosen as 500 Ryd. The convergence criteria chosen were 0.1 μHa for the total energy and 0.1 mHa/Bohr radius for the geometry optimization.

The program FPLO is a full-potential all-electron local-orbital code. It employs a fixed orbital basis with 4f, 5s5p5d5f, 6s6p6d, 7s valence orbitals for Gd and 1s, 2s2p, 3s3p3d valence orbitals for C. The LDA+U approach in the atomic limit version was applied with different values of U (see below) and $J = 0.8$ eV. The LDA functional was parametrized according to Perdew and Zunger.[41]

III. Results and Discussion

A. Structure and Magnetic Ground State. Let us recall that an early structural investigation[23] reported an anomalous endohedral structure of Gd@C_{82} different from previously determined structures of La@C_{82} and Sc@C_{82}. In addition, not the same anomalous structure was suggested by the experiment but yet another one was suggested by DFT calculations.[24−26] However, most recently Liu et al.[28] have shown by XANES that Gd@C_{82} has a normal endohedral structure. Furthermore, Mizorogi and Nagase[27] revealed by DFT calculations that the anomalous structures are unstable.

Our calculations support the findings of the most recent theoretical and experimental investigations. We optimized the geometry of Gd@C_{82} by NWChem and obtained, as expected, a structure with C_{2v} symmetry (see Figure 1), where the Gd atom is situated above the center of a hexagonal carbon ring. The optimized coordinates of the inequivalent atoms can be found in Table 1. The calculated Gd−C bond length is 2.49 Å, while C−C bond lengths amount to 1.46 and 1.49 Å. We repeated the calculations with a more complete basis set (6-31G*). We found a reduction of the Gd−C bond length by about 0.8% (2.47 Å), which is in agreement with ref 27 and a somewhat smaller reduction of the C−C bond lengths (1.46 and 1.48 Å). Since the change in the geometry of the endohedral metallofullerene with the more complete basis set is so small, we performed all further calculations using the structure obtained with the smaller basis set. OpenMX optimization by GGA+U yields a very similar structure where the Gd atom locates at a position slightly off the center of the ring. These OpenMX

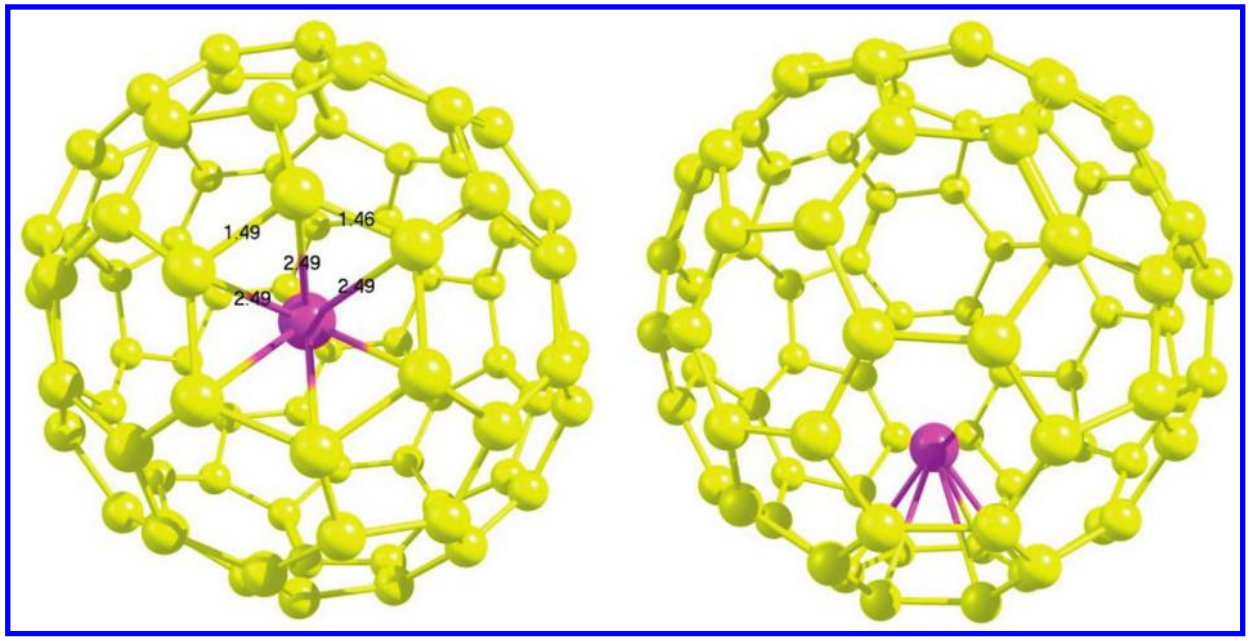

Figure 1. Top and side views of Gd@C_{82} (relaxed structure). Distances are given in Ångstroms.

TABLE 1: Coordinates and Spin Moments for All Inequivalent Atoms of Gd@C_{82}[a]

		coordinates (Å)			spin moments (μ_B)	
number	element	*X*	*Y*	*Z*	$M = 9$	$M = 7$
1	Gd	0.000	0.000	1.822	7.143	7.119
2	C	−1.215	3.943	0.643	0.002	−0.004
3	C	0.000	3.853	1.368	0.000	0.002
4	C	0.000	3.068	2.573	−0.010	−0.003
5	C	1.213	4.018	−0.789	0.025	−0.028
6	C	0.000	3.960	−1.534	−0.005	0.005
7	C	2.387	3.182	1.064	0.032	−0.037
8	C	2.354	2.368	2.217	−0.003	0.006
9	C	1.160	2.363	3.026	0.012	−0.022
10	C	3.108	1.166	2.198	0.000	0.002
11	C	2.408	2.669	−2.458	0.025	−0.028
12	C	2.400	3.325	−1.252	0.007	−0.008
13	C	3.091	2.754	−0.121	−0.001	0.001
14	C	3.687	1.465	−0.207	0.003	−0.003
15	C	3.764	0.720	1.004	0.025	−0.028
16	C	−1.205	2.652	−3.285	−0.005	0.006
17	C	0.000	3.256	−2.829	−0.000	−0.000
18	C	2.661	0.000	2.943	0.016	−0.029
19	C	1.512	0.000	3.803	−0.000	−0.029
20	C	0.743	1.238	3.847	−0.021	−0.017
21	C	3.097	1.406	−2.599	0.034	−0.037
22	C	3.660	0.735	−1.481	0.014	−0.015
23	C	−1.203	−1.426	−4.021	0.035	−0.039
24	C	−2.403	−0.683	−3.638	−0.003	0.004
25	C	0.000	−0.739	−4.330	−0.005	0.006

[a] The coordinates originate from geometry optimization using NWChem with the B3LYP functional. The moments were obtained at the given coordinates by FPLO with LSDA+U using the PZ-81 functional and $U = 8$ eV, $J = 0.8$ eV.

calculations also reveal that the previously suggested two anomalous geometries have 1.7 eV higher energies than the ground state structure.

The magnetic moment of the unpaired electron in the hybrid orbital can couple with that of the seven Gd-4f electrons ferromagnetically or antiferromagnetically. While the parallel arrangement corresponds to $M = 9$, the antiparallel arrangement results in $M = 7$. The measured values of the effective magnetic moment of Gd@C_{82} correspond to the $M = 7$ state. Furukawa et al.[14] found experimentally that the antiferromagnetic arrangement has about 2 meV lower in energy than the ferromagnetic one. On the other hand, Curie−Weiss law fits to experimental data by Huang et al.[12] suggest that the antiferromagnetic arrangement dominates up to room temperature.

We have calculated the energy differences between the two magnetic states in LSDA+U approximation, using the FPLO code. Reasonable values of *U* for 4f states of neutral rare-earth atoms range between 6 and 7 eV.[42] These values are expected to be somewhat enhanced in a cationic situation due to the related orbital contraction. Sabirianov et al. performed similar calculations for Gd@C_{60} and varied *U* from 6 to 7.6 eV. They found[30] best agreement of the occupied 4f levels with the position of photoemission features with strong Gd 4f weight for $U = 7.6$ eV. Here, we considered the range $U = 8$, 10, and

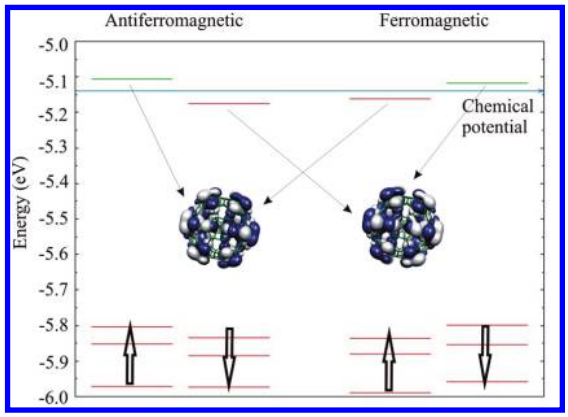

Figure 2. Single electron energy levels of $Gd@C_{82}$ for the antiferromagnetic ($M = 7$) and ferromagnetic ($M = 9$) arrangements, obtained by scalar-relativistic LSDA+U calculations using the FPLO code, $U = 8$ eV. Dark (red online) and light lines (green online) represent occupied and unoccupied electron energy levels, respectively. The dark (blue online) and the light (gray online) areas in the density pictures represent positive and negative values of the related HOMO and LUMO wave function. The Gd contribution is not visible in these pictures, since it amounts to about 1.5% only.

12 eV (note, $J = 0.8$ eV in all cases). All considered values yield an $M = 7$ ground state, in accordance with the experiment. The $M = 9$ state lies 9 (3, 0.3) meV higher in energy than the ground state for $U = 8$ (10, 12) eV. While we think that a value of U close to 8 eV is most justified (in accordance with the value suggested by Sabirianov et al.[30]), we tried the other values in order to check the stability of the magnetic ground state with respect to variation of this parameter. For the sake of completeness, we also performed conventional LSDA and GGA calculations. A conventional LSDA calculation ($U = J = 0$) yields the $M = 9$ state at 90 meV higher energy than the $M = 7$ state. Application of the generalized gradient approximation (PBE version) provides the same order of magnetic states and somewhat smaller energy differences of 80 meV for $U = J = 0$ and of 7 meV for $U = 8$ eV and $J = 0.8$ eV. Hence, the energy difference is not very sensitive to the consideration of density gradient contributions but to the value of U. Recall that two different experiments find the $M = 9$ state about 2 meV[14] and >25 meV[12] higher than the $M = 7$ state.

The spin moments for all inequivalent atoms obtained with $U = 8$ eV are given in Table 1. The influence of spin−orbit coupling and noncollinear spin arrangement on the relative energies of antiferromagnetic and ferromagnetic alignments has been checked with the OpenMX code. Both effects produce only marginal changes and can be neglected. Note, however, the possible effect of magnetic anisotropy on the low-temperature field dependent magnetization of a powder sample; see ref 31.

B. Electronic Structure. The electron energy levels of $Gd@C_{82}$ close to the chemical potential, obtained by the FPLO code in scalar-relativistic mode and using LSDA+U, $U = 8$ eV, are shown in Figure 2 for $M = 7$ and for $M = 9$. There is one almost spin-degenerate level at the chemical potential, well-separated from the next lower occupied and next higher unoccupied levels by about 0.6−0.7 eV. In the $M = 7$ ground state, the HOMO is in the spin-down channel and the LUMO in the spin-up channel. The opposite situation is found in the $M = 9$ state.

The occupied 4f levels (spin-up by definition) are situated at ca. −16 eV, about 11 eV below the chemical potential and outside the displayed energy range in Figure 2. Thus, they are chemically inert and only contribute a spin magnetic moment. The calculated position of the occupied 4f levels agrees with the recent photoemission data of $Gd@C_{60}$ locating the 4f emission at −10 to −11 eV binding energy.[30] The unoccupied 4f-spin-down levels are separated from the 4f-spin-up levels by the sum of exchange splitting (about 5 eV in the Gd-4f shell) and the term $U - J$. Thus, they are situated at ca. −4 eV, about 1 eV above the chemical potential (not displayed).

The 6s and 5d electrons of the Gd atom essentially occupy empty states of the carbon cage, since the chemical potential of the empty cage lies below the Gd chemical potential. However, Mulliken population analysis shows a Gd occupation of $4f^{7.02}5d^{1.16}6s^{0.07}$ in the metallofullerene. The 5d occupation indicates a non-negligible degree of covalency. Indeed, population analysis of the individual π-like molecular orbitals reveals a 5d contribution in the percent range.

What might be more interesting is a 4f contribution of about 1% to the (spin-down) HOMO of the $M = 7$ ground state and to the (spin-down) LUMO of the $M = 9$ state. Such a contribution is not present in the spin-up channel (LUMO of the $M = 7$ ground state and HOMO of the $M = 9$ state), since the 4f-spin-up states are inert. This difference provides an explanation for the experimentally observed and also calculated lower energy of the $M = 7$ state: Due to the position of the unoccupied 4f-spin-down states close to the chemical potential, more variational freedom is available for the spin-down molecular orbitals and their energy is reduced with respect to the spin-up levels, thus favoring a spin-down HOMO and a related antiferromagnetic coupling between the Gd-4f shell and the unpaired electron at the cage. Using a simplifying two-level model, one can roughly estimate the lowering of the spin-down level closest to the chemical potential by interaction with the 4f states:

$$\varepsilon^{\downarrow}_{\mathrm{hyb}} - \varepsilon_{\pi} \approx -\frac{(\varepsilon^{\downarrow}_{4\mathrm{f}} - \varepsilon_{\pi})^2 \left| C^{\downarrow}_{4\mathrm{f}} \right|^2}{\varepsilon^{\downarrow}_{4\mathrm{f}} - \varepsilon_{\pi}}$$

Here, $\varepsilon^{\downarrow}_{\mathrm{hyb}}$ and ε_{π} denote the levels of the 4f-π hybrid and of the pure π state, respectively, $\varepsilon^{\downarrow}_{4\mathrm{f}}$ denotes the position of the empty 4f state, and $|C^{\downarrow}_{4\mathrm{f}}|^2$ denotes the squared 4f contribution to the eigenvector of the hybrid state. The latter amounts to about 1% for $U = 8$ eV. Using $\varepsilon^{\downarrow}_{4\mathrm{f}} - \varepsilon_{\pi} \approx 1$ eV, we arrive at a level lowering on the order of 10 meV, accounting for the calculated energy difference between $M = 7$ and $M = 9$ states, 9 meV. This energy difference is reduced, if U is enhanced but stays positive up to the (unreasonably high) value of $U = 12$ eV. We would like to note that the hybridization between carbon π-states and unoccupied Gd 4f-states was also found to be responsible for the magnetic anisotropy in $Gd@C_{82}$ powder.[31]

A final remark is in place to explain the relative position of HOMO and LUMO in the $M = 9$ state. If $M = 9$ is forced in the calculation, the spin-up molecular orbital at the chemical potential is occupied. The related spin density (mainly situated on the carbon cage; see inset of Figure 2) creates an exchange field that lowers the position of the spin-up level. The same happens in the $M = 7$ case for the spin-down level. Both shifts are due to (unphysical) self-exchange of the unpaired electron on the cage. In the $M = 7$ case, the spin-down level was anyway lower in energy than the spin-up level due to 4f-π hybridization, and self-exchange enhances the splitting between the two levels. In the $M = 9$ case, self-exchange and hybridization effects compete and the level splitting is lower than in the $M = 7$ case. Though the total energy is slightly shifted by the described effect in an unphysical manner, this shift is virtually equal in the M

$= 7$ and in the $M = 9$ state and hence does not influence the energy difference between these states.

IV. Conclusions

The experimentally observed reduction of the $Gd@C_{82}$ magnetic moment with respect to that of a free Gd^{3+} ion is due to antiferromagnetic coupling between the 4f electrons of the Gd atom and the remaining unpaired electron on the hybridized molecular orbital. The reason for this antiferromagnetic coupling is a small hybridization of the unoccupied 4f-spin-down states with the highest occupied carbon π-states. It yields an $M = 7$ ground state that we expect to be generic for all Gd-carbon systems with unpaired electrons. For example, an $M = 7$ ground state has also been found for $Gd@C_{60}$ in a recent calculation.[30] Our results point to an energy difference between the $M = 7$ ground state and the $M = 9$ excited state of the order of 10 meV. While this value is larger than the value 2 meV suggested by spectroscopic data,[14] susceptibility data[12] suggest an even larger value of more than 25 meV. High-temperature susceptibility measurements would be in place to clarify this open point.

Acknowledgment. We like to thank Alexey Popov, Michael Kuz'min, Klaus Koepernik, Helmut Eschrig, Gotthard Seifert, and Lothar Dunsch for discussions. Financial support has been provided by the German Science Foundation via SPP 1145.

References and Notes

(1) Bolskar, R. D.; Benedetto, A. F.; Husebo, L. O.; Price, R. E.; Jackson, E. F.; Wallace, S.; Wilson, L. J.; Alford, J. M. *J. Am. Chem. Soc.* **2003**, *125*, 5471.

(2) Kato, H.; Kanazawa, Y.; Okumura, M.; Taninaka, A.; Yokawa, T.; Shinohara, H. *J. Am. Chem. Soc.* **2003**, *125*, 4391.

(3) Fatouros, P. P.; Corwin, F. D.; Chen, Z.-J.; Broaddus, W. C.; Tatum, J. L.; Kettenmann, B.; Ge, Z.; Gibson, H. W.; Russ, J. L.; Leonard, A. P.; Duchamp, J. C.; Dorn, H. C. *Radiology* **2006**, *240*, 756.

(4) Yang, S.; Fan, L.; Yang, S. *J. Phys. Chem. B* **2004**, *108*, 4394.

(5) Slanina, Z.; Kobayashi, K.; Nagase, S. *Nanotech 2004, Technical Proceedings of the 2004 NSTI Nanotechnology Conference and Trade Show*; Laudon, M., Romanowicz, B., Eds.; Computational Publications: Cambridge, MA, 2004; Vol. 3.

(6) Jones, M. A. G.; Morton, J. J. L.; Taylor, R. A.; Ardavan, A.; Briggs, G. A. D. *Phys. Status Solidi* **2006**, *243*, 3037.

(7) Shimada, T.; Okazaki, T.; Taniguchi, R.; Sugai, T.; Shinohara, H.; Suenaga, K.; Ohno, Y.; Mizuno, S.; Kishimoto, S.; Mizutani, T. *Appl. Phys. Lett.* **2002**, *81*, 4067.

(8) Zhang, E.-Y.; Shu, C.-Y.; Feng, L.; Wang, C.-R. *J. Phys. Chem. B* **2007**, *111*, 14223.

(9) Funasaka, H.; Sugiyama, K.; Yamamoto, K.; Takahashi, T. *J. Phys. Chem.* **1995**, *99*, 1826.

(10) Kessler, B.; Bringer, A.; Cramm, S.; Schlebusch, C.; Eberhardt, W.; Suzuki, S.; Achiba, Y.; Esch, F.; Barnaba, M.; Cocco, D. *Phys. Rev. Lett.* **1997**, *79*, 2289.

(11) Kobayashi, K.; Nagase, S. *Chem. Phys. Lett.* **1998**, *282*, 325.

(12) Huang, H.; Yang, S.; Zhang, X. *J. Phys. Chem. B* **2000**, *104*, 1473.

(13) Suenaga, K.; Iijima, S.; Kato, H.; Shinohara, H. *Phys. Rev. B* **2000**, *62*, 1627.

(14) Furukawa, K.; Okubo, S.; Kato, H.; Shinohara, H.; Kato, T. *J. Phys. Chem. A* **2003**, *107*, 10933.

(15) De Nadaï, C.; Mirone, A.; Dhesi, S. S.; Bencok, P.; Brookes, N. B.; Marenne, I.; Rudolf, P.; Tagmatarchis, N.; Shinohara, H.; Dennis, T. J. S. *Phys. Rev. B* **2004**, *69*, 184421.

(16) Bondino, F.; Cepek, C.; Tagmatarchis, N.; Prato, M.; Shinohara, H.; Goldoni, A. *J. Phys. Chem. B* **2006**, *110*, 7289.

(17) Kitaura, R.; Okimoto, H.; Shinohara, H.; Nakamura, T.; Osawa, H. *Phys. Rev. B* **2007**, *76*, 172409.

(18) Nishibori, E.; Takata, M.; Sakata, M.; Inakuma, M.; Shinohara, H. *Chem. Phys. Lett.* **1998**, *298*, 79.

(19) Nishibori, E.; Takata, M.; Sakata, M.; Tanaka, H.; Hasegawa, M.; Shinohara, H. *Chem. Phys. Lett.* **2000**, *330*, 497.

(20) (a) Akasaka, T.; Wakahara, T.; Nagase, S.; Kobayashi, K.; Waelchli, M.; Yamamoto, K.; Kondo, M.; Shirakura, S.; Okubo, S.; et al. *J. Am. Chem. Soc.* **2000**, *122*, 9316. (b) Tsuchiya, T.; Wakahara, T.; Maeda, Y.; Akasaka, T.; Waelchli, M.; Kato, T.; Okubo, H.; Mizigori, N.; Kobayashi, K.; Nagase, S. *Angew. Chem., Int. Ed.* **2005**, *44*, 3282.

(21) Akiyama, K.; Sueki, K.; Kodama, T.; Kikuchi, K.; Ikemoto, I.; Katada, M.; Nakahara, H. *J. Phys. Chem. A* **2000**, *104*, 7224.

(22) Giefers, H.; Nessel, F.; Györy, S. I.; Strecker, M.; Wortmann, G.; Grushko, Yu. S.; Alekseev, E. G.; Kozlov, V. S. *Carbon* **1999**, *37*, 721.

(23) Nishibori, E.; Iwata, K.; Sakata, M.; Takata, M.; Tanaka, H.; Kato, H.; Shinohara, H. *Phys. Rev. B* **2004**, *69*, 113412.

(24) Senapati, L.; Schrier, J.; Whaley, K. B. *Nano Lett.* **2004**, *4*, 2073.

(25) Wang, L.; Yang, D. *Nano Lett.* **2005**, *5*, 2340.

(26) Senapati, L.; Schrier, J.; Whaley, K. B. *Nano Lett.* **2005**, *5*, 2341.

(27) Mizorogi, N.; Nagase, S. *Chem. Phys. Lett.* **2006**, *431*, 110.

(28) Liu, L.; Gao, B.; Chu, W.; Chen, D.; Hu, T.; Wang, C.; Dunsch, L.; Marcelli, A.; Luo, Y.; Wu, Z. *Chem. Commun.* **2008**, 474.

(29) Richter, M. *J. Phys. D: Appl. Phys.* **1998**, *31*, 1017.

(30) Sabirianov, R. F.; Mei, W. N.; Lu, J.; Gao, Y.; Zeng, X. C.; Bolskar, R. D.; Jeppson, P.; Wu, N.; Caruso, A. N.; Dowben, P. A. *J. Phys.: Condens. Matter* **2007**, *19*, 082201.

(31) Mirone, A. *Eur. Phys. J. B* **2005**, *47*, 509.

(32) Bylaska, E. J.; de Jong, W. A.; Kowalski, K.; Straatsma, T. P.; Valiev, M.; Wang, D.; Apra, E.; Windus, T. L.; Hirata, S. *NWChem, A Computational Chemistry Package for Parallel Computers, Version 5.0*; Pacific Northwest National Laboratory: Richland, WA, 2006.

(33) Koepernik, K.; Eschrig, H. *Phys. Rev. B* **1999**, *59*, 1743. (http://www.fplo.de).

(34) (a) Ozaki, T. *Phys. Rev. B* **2003**, *67*, 155108. (b) Ozaki, T.; Kino, H. *Phys. Rev. B* **2004**, *69*, 195113.

(35) Ozaki, T.; Kino, H. *Phys. Rev. B* **2005**, *72*, 045121.

(36) Becke, A. D. *J. Chem. Phys.* **1993**, *98*, 5648.

(37) Cundari, T. R.; Stevens, W. J. *J. Chem. Phys.* **1993**, *98*, 5555.

(38) Troullier, N.; Martins, J. L. *Phys. Rev. B* **1991**, *43*, 1993.

(39) Han, M. J.; Ozaki, T.; Yu, J. *Phys. Rev. B* **2006**, *73*, 045110.

(40) Perdew, J. P.; Burke, K.; Ernzerhof, M. *Phys. Rev. Lett.* **1996**, *77*, 3865.

(41) Perdew, J. P.; Zunger, A. *Phys. Rev. B* **1981**, *23*, 5048.

(42) Richter, M. Density functional theory applied to 4f and 5f elements and metallic compounds. In *Handbook of Magnetic Materials*; Buschow, K. H. J., Ed.; Elsevier: Amsterdam 2001; Vol. 13, pp 87−228.

JP906243V